the volume is expressed in terms of these parameters in Eq. (6) of Ref 1, it would be desirable to also utilize these variables in the expression for weight.

Combining Eqs. (7) and (8) of Ref 1

$$W_{BB} = \frac{\rho p b^3 C_R}{6 h_R f}\left[\frac{\lambda}{8} + \frac{(1-\lambda)}{24}\right] k_{ib} \tag{1}$$

Substituting

$$b^2 = ARS \tag{2}$$

$$p = Wn/S \tag{3}$$

into Eq. (1),

$$W_{BB} = \frac{WnAR^{3/2}S^{1/2}\rho}{6(h_R/C_R)f}\left[\frac{\lambda}{8} + \frac{(1-\lambda)}{24}\right] k_{ib} \tag{4}$$

Now, if variations in wing weight under constant performance conditions are being considered, the wing loading, as given by Eq. (3), will be constant, and under another performance requirement the aspect ratio may be constant; we have

$$W_{BB} = \frac{\rho K A R^{3/2} S^{3/2}}{6(h_R/C_R)f}\left[\frac{\lambda}{8} + \frac{(1-\lambda)}{24}\right] k_{ib} \tag{5}$$

$$W/S = K$$

or

$$W_{BB} = \frac{\rho A R^{3/2} W^{3/2}}{6(h_R/C_R) f K^{1/2}}\left[\frac{\lambda}{8} + \frac{(1-\lambda)}{24}\right] k_{ib} \tag{6}$$

The total wing weight can be expressed as

$$W_w = W_{BB} + K_1 S \tag{6a}$$

where the secondary structure weight is shown to be proportional to wing area. The volume, given by Eq. (6) of Ref 1, may be expressed in terms of gross weight:

$$\frac{K^{3/2} V A R^{1/2}}{W^{3/2}} = \frac{0.67 r\phi}{(1+\lambda)^2}\left\{\lambda^2 (t/c)_t + (t/c)_R + \lambda[(t/c)_t (t/c)_R]^{1/2}\right\} \tag{7}$$

and the wing weight may be expressed in terms of the volume:

$$W_{BB} = \frac{K\rho A R^2 (1+\lambda)^2\{(\lambda/8) + [(1-\lambda)/24]\} k_{ib} V}{4(h_R/c_R) f r\phi\{\lambda^2 (t/c)_t + (t/c)_R + \lambda[(t/c)_t (t/c)_R]^{1/2}\}} \tag{8}$$

Equation (8) shows how wing weight varies with wing volume when performance requires wing loading and aspect ratio to remain constant. As a refinement, it is noted that the stress f is independent of chord loading for tension loadings, such as is the case for the wing lower surface where a stress level is specified for fatigue requirements; but it is to be recognized that the stress will vary with chord loading when compressive stresses are critical.

Now, considering box beams that are critical for torsional stiffness requirements, we can write

$$\theta = \int_0^{b/2} \frac{T dy}{GJ} \tag{9}$$

$$W_{BB} = \int_0^{b/2} st dy \tag{10}$$

For wings of moderate or large aspect ratios it can be shown that

$$W_{BB} \propto \frac{AR^2}{(h/c)^2} \tag{11}$$

As an example, for a constant wing geometry and constant torque,

$$\theta = T b_s / 8 G A^2 t \tag{12}$$

and

$$W_{BB} = s\left[\frac{T b_s}{8 G \theta A^2}\right]\frac{b}{2} = \frac{1}{4G\theta}\left(\frac{b}{c}\right)^2\left(\frac{c+h}{h}\right)^2 = \frac{1}{4G\theta} AR_{\text{BOX}}^2 \frac{(1+h/c)^2}{(h/c_{\text{BOX}})^2} \tag{13}$$

Letting

$$(h/c)_{\text{BOX}} = K_1 (h/c)_{\text{WING}} \qquad AR_{\text{BOX}} = K_2 (h/c)_{\text{WING}}$$

Eq. (12) can be written as

$$W_{BB} = \frac{K_2^2 AR_{\text{WING}}^2}{4G\theta K_1^2}\frac{(1+h/c)^2}{(h/c_{\text{WING}})^2} \tag{14}$$

which is of the form given by Eq. (11).

For low-aspect ratio wings in which warpage restraints are more severe, a somewhat different analysis would be required in order to obtain the relationship for stiffness critical wings.

Reference

[1] Saelman, B., "Effect of wing geometry on volume and weight," J. Aerospace Sci. 29, 1390–1392 (1962).

Design of the Bubbler Ozone Detector

M. Griggs*
General Dynamics/Astronautics, San Diego, Calif.

Introduction

It has long been desirable to have a simple and cheap method for measuring the vertical distribution of atmospheric ozone. If this is measured on a widespread regular basis, using the quasi-conservative property of ozone in the lower stratosphere, the results will be of considerable value in understanding the dynamic processes in the atmosphere. This led to the development of the bubbler ozonesonde. It is simple in design and use, gives an absolute measurement of ozone, and is cheap to produce. It has been used on many balloon flights in different parts of the world. A laboratory model has been built, but this description is limited to the balloon-borne detector.

Principle of the Bubbler

The method of detecting the ozone relies on the familiar reaction of ozone with potassium iodide solution to form free iodine. This iodine is measured by the passage of a current between two electrodes, one platinum, the other silver, immersed in the solution. The cell has a spontaneous emf that is balanced by an applied emf of about 0.43 v.

The air and ozone are bubbled through the solution, and the ozone is removed according to the equation

$$2KI + O_3 + H_2O \rightarrow 2KOH + I_2 + O_2 \tag{1}$$

Presented as Preprint 64-321 at the AIAA 1st Annual Meeting, Washington, D. C., June 29–July 2, 1964; revision received August 6, 1964. The development of this instrument was done at the Clarendon Laboratory, Oxford, England, under a grant from the Gassiot Committee of the Royal Society. The author would like to thank A. W. Brewer, now at Toronto University, for advice and encouragement in this work.

* Staff Scientist, Space Science Laboratory.

The iodine reaches the platinum cathode by the mixing action of the bubbling, and the iodide ion is formed:

$$I_2 + 2e \rightarrow 2I^- \quad (2)$$

This iodide ion is then removed from the solution at the silver anode to form silver iodide that is practically insoluble:

$$2I^- - 2e + 2Ag \rightarrow 2AgI \quad (3)$$

It is seen that for each ozone molecule entering the solution, two electrons pass through the cell and external circuit. Thus, the current from the cell gives a direct and continuous measurement of the ozone content of the air being bubbled through the solution. For the airflow rates (about 150 ml/min) used, and typical atmospheric concentrations of ozone, this current varies between 0 and 7μa, which is easily measured.

The reaction of ozone with potassium iodide solution has been thoroughly examined in the past.[1, 2] The oxidation of KI solution is not specific to ozone. However, the other atmospheric constituents that will liberate iodine from KI solution have slow reactions, and it has been shown that only NO_2 is likely to be effective in neutral KI solution. Even then, NO_2 is only 2% as efficient as ozone in liberating iodine. Equation (1) is stoichiometrically correct only in neutral KI solution. The neutrality of the solution in the bubbler is maintained by a phosphate buffer, consisting of 0.1% solutions of sodium hydrogen phosphate and disodium hydrogen orthophosphate.

A description of some of the operating characteristics of the bubbler is given by Brewer and Milford.[3]

Design of the Bubbler

In the original design for the bubbler (Fig. 1a), the air was sucked through the bubbler. However, it was seen that much simplification in construction could be achieved if the air were blown through the solution, passing through the pump before entering the solution. The final design is shown in Fig. 1b.

This system has several advantages:

1) An airtight system is not needed. This is the main advantage, as the bubbler does not have to be opened up to be filled with solution and then sealed before use at an ozonesonde station.

2) Construction is simplified, and the vapor trap, which is necessary to prevent water vapor being drawn into the sucking pump, is eliminated.

3) The pump, which is a constant displacement piston pump, will work at lower ambient pressures when in the blowing mode. In the sucking mode, the sucking force is limited by the solution vapor pressure becoming comparable to the ambient atmospheric pressure.

The only disadvantage of this system (and it would appear to be a big one) is that ozone will be destroyed as the air passes through the pump. However, by careful choice of pump materials, lubricants, and materials for the bubbler itself, the ozone losses have been kept to less than 8%. It is better to have a known loss of 4% ± 4% than to risk an incorrect ozone reading of unknown error due to faulty seals in the sucking system.

The diagram of the bubbler is self-explanatory, but some comments on detail are given. The dimensions of the cell are chosen so that optimum response time and complete ozone extraction are obtained. The length *CD* above the cell is made sufficiently long, so that bubbles of solution carried up the side of the bubbler burst before reaching the open top. The cap of the bubbler is designed so that the bubbler may be inverted without spilling the 2 ml of solution.

The platinum gauze cathode is kept slightly away from the walls of the cell by ribs on the side and a projection at the bottom of the cell. This is essential so that there can be free flow of solution through the gauze, which is desirable for a good response time of the bubbler. The silver wire anode is taken upwards in a groove between two of the ribs. The anode is arranged in this position because it was found that, when coiled beneath the platinum cup as in the prototype, a bubble of air could form in the small space below the gauze, thus isolating the anode from the solution and preventing the passage of a current.

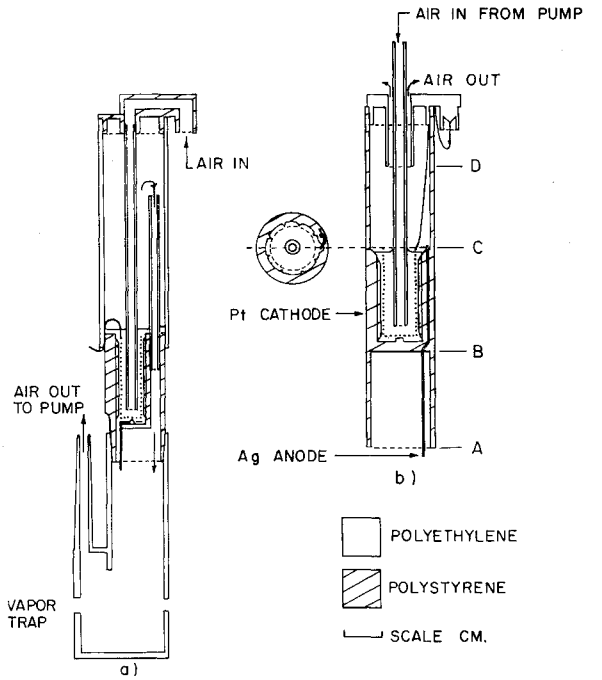

Fig. 1 a) Prototype sucking bubbler, b) blowing bubbler.

Choice of Materials Used in the Bubbler

The materials used in the construction of the bubbler system can cause inaccurate ozone readings in two ways. Ozone may be reduced in the intake system before it reaches the solution in the reaction cell; secondly, iodine, formed by the ozone reacting with the solution, may be absorbed by the walls of the reaction cell. To minimize these effects, the materials for the pump and the bubbler were carefully chosen after investigating ozone and iodine absorption properties of different plastics.

The bubbler designed for the ozonesonde is constructed in plastic so that the components may be cheaply produced on a large scale. The original fabrication of the bubbler components was done with a small hand-operated injection moulding machine. This limited the choice of materials to thermoplastics. In addition, they had to be cheap, readily available, and structurally suitable for the job. For example, not all thermoplastics are suitable for withstanding the wear on the pump.

The ozone and iodine absorptions by different materials were determined with a laboratory model of the bubbler constructed of glass. This bubbler was compared with the standard sodium thiosulphate method of measuring ozone and proved to measure ozone accurately, without any losses.

To measure the ozone absorption by a material, the output from a constant ozone supply was bubbled through the glass bubbler; the change in the bubbler output current was determined when a sample of the material was placed in the inlet of the bubbler. This was done for plastics suitable for construction of the bubbler inlet system and the pump and for lubricating oils for the pump.

To determine the iodine absorption by a material, the change in output of the glass bubbler was measured when a sample of the material was dropped into the reaction cell.

The results of the tests are shown in Table 1. On the basis of these results, the reaction cell is made of polystyrene, the inlet tubes of polyethylene, and the pump of cellulose acetate.

Table 1 Absorption of ozone and iodine[a]

Materials		Oils
Ozone	Iodine	Ozone
Glass	Glass	Watch oil
Acetate	Polystyrene	Apiezon A oil
Nylon	Acetate	Florube oil
Polyethylene	Polyethylene	Silicon oil
Polyvinyl chloride	Perspex	
	Polyvinyl chloride	
	Nylon	

[a]The columns show the materials in order of suitability for use with the bubbler. The material absorbing least heads the column.

The best lubricating oil for the pump was, surprisingly, a simple watch oil.

In the final manufacture of the bubbler and pump, great care is taken to keep all the components clean, and certain treatments are carried out to help further reduce losses. The pumps and polyethylene tubing are stored in a permanent ozone atmosphere, and the lubricating oil is regularly ozonized by bubbling ozone through it for several hours. Iodine absorption losses are reduced by iodization of the bubbler reaction cell. It is filled with potassium iodide solution, and ozone is bubbled through it to form iodine. This is not removed electrochemically, and the walls of the cell are allowed to absorb the iodine.

These treatments proved very effective. Ozonesondes treated this way and stored in conditions similar to those at an ozonesonde station were found to have ozone losses ranging from 0 to 7%. As a result, the total ozone losses in an ozonesonde sounding are assumed to be $4 \pm 4\%$.

Accuracy of the Bubbler Ozonesonde

In addition to the ozone and iodine losses just mentioned, there are errors involved in monitoring the airflow rate during the ozonesonde sounding. These errors are $\pm 6\%$, giving a total possible error of $\pm 10\%$ before telemetry, which may introduce further errors. However, analysis of more than fifty ozonesonde flights in England suggests that the errors are probably less.

References

[1] Bowen, I. G. and Regener, V. H., "On the automatic chemical determination of atmospheric ozone," J. Geophys. Res. **56**, 307–324 (1951).

[2] Glackauf, E., Heal, H. G., Martin, G. R., and Paneth, F. A., "A method for the continuous measurement of the local concentration of atmospheric zone," J. Chem. Soc., 1–4 (1944).

[3] Brewer, A. W. and Milford, J. R., "The Oxford-Kew ozonesonde," Proc. Roy. Soc. (London) **A256**, 470–495 (1960).

Trailing Vortices of Jet Transport Aircraft during Takeoff and Landing

EDGAR L. ZWIEBACK*
Douglas Aircraft Company, Inc., Long Beach, Calif.

RECENTLY, emphasis has been placed on determining the minimum safe separation intervals of aircraft during approach, landing, and takeoff from busy airports. One of the limiting factors governing the separation interval is the wing trailing vortex velocity field of the lead aircraft. This vortex velocity field affects the separation interval somewhat as the type and size vary of the lead and following aircraft. In addition, the movements of the trailing vortices result in different exposure paths for the following aircraft, depending on whether a takeoff or landing is being conducted. Multiple runway layouts involve considerations of trailing vortex movement. Parallel runways require sufficient lateral separation to prevent trailing vortices generated over one runway from interfering with operations at the adjacent runway. Intersecting runways are continuously subject to trailing vortex interference. For example, a long main runway, reserved for very large airplanes, may intersect several short runways used for general aviation operations, and therefore the very large airplane trails vortices over all the intersecting runways used by light aircraft. The induced effects of the trailing vortices have become more serious with the advent of the large jet transport aircraft capable of creating very strong vortices. Recently, several cases of litigation have been noted in which it was claimed that fatal airplane crashes were the result of taking off into a trailing vortex velocity field generated by large jet transports.

The danger of trailing vortices to light planes during takeoff and landing has been attested to by almost all of the Douglas Aircraft Company pilots, flying light twin-engined aircraft into airports used by large jet transports. In particular, jet transport training operations where the light aircraft follow the large transport, making touch-and-go landings, results in trailing vortices occurring along the entire runway. Numerous causes of uncontrollable 90° to 180° rolls in 6000-lb aircraft have been experienced by Douglas Company pilots encountering trailing vortices, and the usual experience has been that the vortex velocity field will force the aircraft out of the vortex in a few seconds. As the aircraft may be inverted when coming out of the vortex, encountering vortices near the ground must be avoided.

In order to obtain quantitative information on the behavior of trailing vortices of jet transports near the ground, the Systems Research and Development Service of the Federal Aviation Agency sponsored a test program, and this note will present data from this program on the movement and decay of wing trailing vortices from Douglas DC-8 jet transport aircraft during takeoff and landing in low wind conditions. The complete test program and data are detailed in Ref. 1. Existing theory will be used to show the degree of correlation with the test data. The difference in wing configuration for the DC-8 during takeoff and landing results in a large increase in flap-end vorticity during landing. Information on the number of trailing vortices will be presented for both configurations. The test program was conducted in two parts. Each of the parts and its results will be described separately.

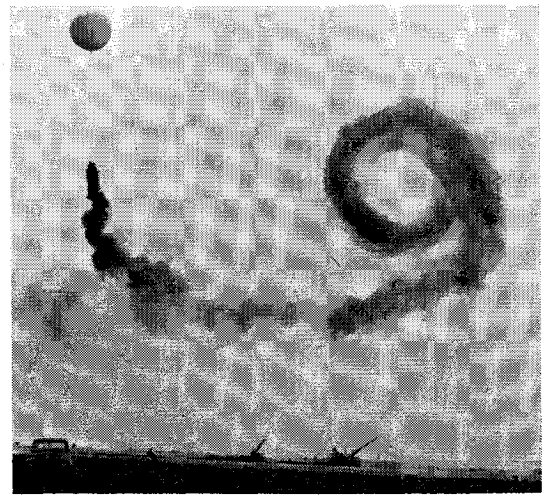

Fig. 1 Wing trailing vortex visualization.

Presented as Preprint 64-325 at the AIAA 1st Annual Meeting, Washington, D. C., July 2, 1964; revision received August 24, 1964.

* Flight Test Research Engineer, Flight Development, Aircraft Division. Member AIAA.